Kinetics of the Thermal Decomposition of Alum Sourced from Kankara Kaolin

[1]Olubajo O. O., [2]S. M. Waziri, [2]B. O. Aderemi

[1]Department of Chemical Engineering, Abubakar Tafawa Balewa University Bauchi, Nigeria
[2]Department of Chemical Engineering, Ahmadu Bello University, Zaria, Nigeria

***ABSTRACT*- This study investigated the kinetics of the thermal decomposition of alum produced from Kankara kaolin. The work involved preparation of alum as well as calcination of the prepared alum. The Coats-Redfern kinetic model was adopted in estimating the kinetic parameters for the decomposition reactions. The experiment was conducted using a muffle furnace and the rate data were obtained using thermogravimetric (TG) and Xray fluorescence (XRF) analyses. From the TGA experimental data, an average order of reaction, n of 1.3 with corresponding activation energy value of 321.03 kJ/molK and frequency factor 2.57E+14min^{-1} gave the smallest residual deviation values and best fitting curves compared to other reaction orders tested within the range of 0 to 2, while equivalent values from XRF residual sulphate data are n = 1, activation energy = 337.22 kJ/molK and frequency factor of 5.27E+14 min^{-1}. The discripances in the corresponding values from the two modes of data generation is attributed to the differences in the reaction mechanisms captured by the different methods of analysis. While, the XRF solely followed the sulfate decomposition phenomenon, TGA was more encompassing including dehydroxylation and impurity decomposition reactions.**

(KEYWORDS: Kankara Kaolin, decomposition, Coats-Redfern model, TGA, XRF, kinetics)

I. INTRODUCTION

The great interest in alumina is mostly due to its ever increasing applications as adsorbents, catalysts support, refractory, filler and as constituents of various household products. Invariably, bauxite has been the dominant source alumina, through the popular Bayer's process [1]. However, notwithstanding the acclaimed bauxite's relative economic advantages over all other alternative sources, its rapid depletion in quantity and quality globally is an impetus promoting intensive research activities on alumina extraction from clay materials worldwide [2]. In fact, this is a welcome development to many countries such as Nigeria that are not naturaly endowed with bauxite but having kaolin in abundance.

It must be admitted that in the last decade, a lot of research efforts have been expended in producing alums, alumina and silica for various purposes from Kankara kaolin clay [3-8]. However, it is of note that while much of the efforts were geared towards establishing favourable process conditions, apparently, no such attention has been paid to the prevailing kinetics.

The work of Moselhy et al. (1994) [9] , on thermal treatment of aluminium sulfate hydrate made a fundamental contribution in addressing the peculiarity of alum decomposition including the testfitting of the Coat-Redfern kinetic model. However, they limited their consideration to only the ideal solid-state reaction cases of order n= ½, 2/3 and 1, thus ignoring the obvious peculiarity of alum. At the onset, it is obvious that a well crystalline alum behaves as a non porous material, in which the shrinking core reaction model ought to describe, howbeit, as reaction progresses and it is evacuated of the occluded free water and sulfate ions, it becomes a porous material to mimic a diffusion-progressive phenomenon. Even at that, decomposition of alum to release the bonded waters (water of crystallization) requires different energy level (activation energy) to that of sulfate decomposition, with no clear cut demarcation in time or space of the occurence of these duo phenomena.

The strenght of the Coat-Redfern model resides in its development, which is free from the majority of the idealized models assumptions. It equally merged the kinetic constants with the thermodynamic parameters in a single equation, thus affording the evaluation of reaction order, activation energy and reaction frequency factor from same set of data. Its major shortcoming being that the order of reaction determination, inherently depends on the trial and error principle, whether by numerical or graphical approach.

The use of thermogravimetric data to evaluate kinetic parameters for solid state reactions involving weight loss has been investigated by a number of workers as noted by Coats and Redfern (1964) [10] , but sad enough, the single sample, rapid, and continous kinetics calculation over the entire temperature range offered by dynamic thermogravimetry is still not executable in Nigeria, five decades after, due to lack of requisite thermo-balance facility in the neighborhood.

Hence, this paper attempts to estimate the kinetic parameters such as activation energy, pre-exponential factor and the order of reaction using Coats-Redfern kinetic model. Therefore, the present work attempts to explore the traditional cumbersome isothermal gravimetry under varying holding time and temperature. The study also involves the preparation of single alum from local clay and the calcination of the produced alum at various temperatures and holding times. Gravimetric determination was employed in monitoring the overall rate data, while X-ray Fluorescence analyses of the residual sulfate concentration in the alumina were obtained to model sulphate decomposition specifically.

Derivation of Coat-Redfern Model

In general, for the reaction $aA_{(s)} \rightarrow bB_{(s)} + cC_{(g)}$ the disappearance of component A can be described by the formal kinetic expression:

$$\frac{\mathrm{dX}}{\mathrm{dt}} = \mathrm{kf(X)} \tag{1a}$$

$$\frac{\mathrm{dX}}{\mathrm{dt}} = Ae^{-E/RT}\mathrm{f(X)} \tag{1b}$$

From Arrhenius,

$$k = Ae^{-E/RT} \tag{2}$$

Where X is the fractional conversion; t is the time; A is the pre-exponential factor; E is the activation energy; R is the gas constant; T is the temperature in Kelvin and f (X) is the kinetic function which takes different forms depending on the particular reaction rate equation. In isothermal kinetic studies, the rate equation used to calculate the rate constant has the form:

$$\mathrm{g(X)} = k\,\mathrm{t} \tag{3}$$

Differentiating with respect to time t

$$\frac{\mathrm{d[g(X)]}}{\mathrm{dt}} = k \tag{4}$$

Substituting the LHS term of Equation 4 into Equation 1a to give

$$\frac{\mathrm{d[g(X)]}}{\mathrm{dt}}\mathrm{f(X)} = \frac{dX}{dt} \tag{5}$$

$$\mathrm{d[g(X)]}f\mathrm{(X)} = dX \tag{6}$$

Making $d[g(X)]$ subject of the formula

$$d\mathrm{[g(X)]} = {}^{dX}/_{f(X)} \tag{7}$$

Integrating with respect to X

$$\mathrm{g(X)} = \int_0^X dX\,/\,f(X) \tag{8}$$

However, non-isothermal methods are becoming more widely used because they are more realistic than the classical isothermal methods. In non-isothermal kinetics the time dependence on the left hand side of Equation 1 is eliminated using constant heating rate $\beta = \frac{\mathrm{dT}}{\mathrm{dt}}$ so that $\mathrm{T} = \mathrm{T_o} + \beta$, where $\mathrm{T_o}$ is the starting temperature and t is the time of heating. Using integral methods of analysis, from Equation 1:

$$\frac{\mathrm{dX}}{\mathrm{dt}} = \frac{\mathrm{dX}}{\mathrm{dT}}\cdot\frac{\mathrm{dT}}{\mathrm{dt}} = \frac{\mathrm{dX}}{\mathrm{dT}}\cdot\beta \tag{9}$$

Substituting Equation 9 into 1 and making dX/dt, the subject of the formula

$$\frac{\mathrm{dX}}{\mathrm{dT}} = \frac{\mathrm{dX}}{\mathrm{dt}}\cdot\frac{1}{\beta} = {}^{A}/_{\beta}\,e^{-E/RT}f\mathrm{(X)} \tag{10}$$

$$\mathrm{dX} = {}^{A}/_{\beta}\,e^{-E/RT}f\mathrm{(X)dT} \tag{11}$$

$$\mathrm{g(X)} = \int_0^X dX\,/\,f(X) = {}^{A}/_{\beta}\,e^{-E/RT}\,{}^{f\mathrm{(X)dT}}/_{f\mathrm{(X)}} \tag{12}$$

$$\mathrm{g(X)} = \int_{T_o}^{T} {}^{A}/_{\beta}\,e^{-E/RT}\,dT = {}^{A}/_{\beta}\int_{T_o}^{T} e^{-E/RT}\,dT \tag{13}$$

From calculus:

$$e^{ax}\,\mathrm{dX} = {}^{1}/_{\mathrm{a}}\,e^{ax}$$

Therefore, if

$$a = -{}^{E}/_{R} \quad and \quad x = {}^{1}/_{T}$$

Differentiating the above with respect to temperature T gives

$$^{\mathrm{dx}}/_{\mathrm{dt}} = \mathrm{T}^{-2} \Rightarrow \mathrm{dT} = \mathrm{T}^{2}\mathrm{dx}$$

Substituting $\mathrm{dT} = \mathrm{T}^{2}\mathrm{dx}$ into Equation13:

$$^{A}/_{\beta}\int_{T_o}^{T} e^{-E/RT}\,dT = {}^{A}/_{\beta}\int_0^x e^{ax}T^2\,dx = {}^{A}/_{\beta}\int_0^x {}^{e^{ax}}/_{x^2}\,dx \tag{14}$$

Since $e^{ax}\,\mathrm{dx} = {}^{1}/_{\mathrm{a}}\,e^{ax}$

Then using integration by part

$$\int I\;II = I\int II - \int I'\int II \tag{15}$$

Let $I = {}^{1}/_{x^2}$ *and* $II = e^{ax}$, then from Equation 14

$$^{A}/_{\beta}\int_0^x {}^{e^{ax}}/_{x^2}\,dx = {}^{A}/_{\beta}\left[{}^{1}/_{x^2}\int_0^x e^{ax}\,dx + 2\int_0^x {}^{1}/_{x^3}\int_0^x e^{ax}\,dx\right] \tag{16a}$$

$$^{A}/_{\beta}\textstyle\int_0^x {}^{e^{ax}}/_{x^2}\,dx = {}^{A}/_{\beta}\left[{}^{e^{ax}}/_{ax^2} + {}^{2}/_{a}\int_0^x {}^{e^{ax}}/_{x^3}\right] \tag{16b}$$

Taken the integration by part a step further and rewrite Equation 16

$$^{A}/_{\beta}\left[{}^{e^{ax}}/_{ax^2} + {}^{2}/_{a}\int_0^x {}^{e^{ax}}/_{x^3}\right] = {}^{A}/_{\beta}\begin{bmatrix} {}^{e^{ax}}/_{ax^2} + {}^{2}/_{ax^3}\cdot{}^{e^{ax}}/_{a} \\ + {}^{3}/_{a}\int_0^x {}^{e^{ax}}/_{x^4}\,dx \end{bmatrix} \tag{17}$$

It's obvious that the integration continues endlessly, however, from the generic definition of x = 1/T, x^4 and above goes to zero, rendering the equation undefined. Therefore, it becomes expedient to stop at the second term on the right hand bracket.

Hence,

$$\frac{A}{\beta}\left[\frac{e^{ax}}{ax^2}+\frac{2}{a}\int_0^x \frac{e^{ax}}{x^3}\right] \cong \frac{A}{\beta}\left[\frac{e^{ax}}{ax^2}+\frac{2}{ax^3}\cdot\frac{e^{ax}}{a}\right] \qquad (18)$$

Substituting $a = -{}^{E}/_{R}$ and $x = {}^{1}/_{T}$ into Equation 18 gives Equation 19

$$g(X) = \frac{A}{\beta}\left[\frac{-RT^2}{E}e^{-E/RT}\right]_{\infty}^{T} + \frac{A}{\beta}\left[\frac{2R^2T^3}{E^2}e^{-E/RT}\right]_{\infty}^{T} \qquad (19)$$

And then factorize Equation 19 to give Equation 20

$$= -{}^{A}/_{\beta}\left[{}^{RT^2e^{-E/RT}}/_{E}\,(1 - {}^{2RT}/_{E})\right] \qquad (20)$$

$$\therefore\ g(X) = -{}^{A}/_{\beta}\left[{}^{RT^2e^{-E/RT}}/_{E}\,(1 - {}^{2RT}/_{E})\right] \qquad (21)$$

Incorporating the power law Equation 21 as follows:

$$f(X) = (1-X)^{n}\text{, then } g(X) = \int_0^X {}^{dX}/_{f(X)}$$

$$\int_0^X {}^{dX}/_{(1-X)^{n}} = \int_0^X (1-X)^{-n}\,dX \qquad (22)$$

If Equation 22 was integrated to give:

$$\therefore\ g(X) = \left[\int_0^X 1-(1-X)^{1-n}/_{1-n}\right] \qquad (23)$$

Substituting Equation 23 into Equation 21

$$g(X) = -\left[\frac{1-(1-X)^{1-n}}{(1-n)}\right] = \frac{-ART^2(1-{}^{2RT}/_{E})}{\beta E}e^{-E/RT} \qquad (24)$$

Dividing Equation 24 through by T^2

$$\frac{g(X)}{T^2} = -\left[\frac{1-(1-X)^{1-n}}{T^2(1-n)}\right] = -{}^{AR}/_{\beta E}\,(1-{}^{2RT}/_{E})e^{-E/RT} \qquad (25)$$

Taking the negative natural logarithm of both sides

$$-In\left[\frac{g(X)}{T^2}\right] = In\left[\frac{1-(1-X)^{1-n}}{T^2(1-n)}\right] = \text{In}\frac{AR}{\beta E}\left(1-\frac{2RT}{E}\right) + {}^{E}/_{RT} \qquad (26)$$

The equation has been written in the form:

$$-In\left[\frac{g(X)}{T^2}\right] = In\left[\frac{1-(1-X)^{1-n}}{T^2(1-n)}\right] = \text{In}\frac{AR}{\beta E}\left(1-\frac{2RT}{E}\right) + {}^{E}/_{RT} \qquad (27)$$

Equation 27 satisfies for $n < 1$or $n > 1$ but for $n=1$, Equation 27 becomes

$$-In\left[\frac{g(X)}{T^2}\right] = In\left[\frac{-In(1-X)}{T^2}\right] = \text{In}\frac{AR}{\beta E}\left(1-\frac{2RT}{E}\right) + {}^{E}/_{RT} \qquad (28)$$

For Equations 27 and 28 to be amenable to graphical solution, the quantity $\left(1-\frac{2RT}{E}\right)$ is assumed to be close to 1, hence the need to verify the reasonability of this assumption [10].

II. MATERIALS

Raw kaolin used in this investigation was obtained from Kankara village, Katsina State, Nigeria, while beneficiated and metakaolin were obtained from processing of the raw clay and calcination of the beneficiated clay respectively. Fresh alum produced in this work as described in the following subsection meets general requirement of 6-9% wt of Al_2O_3/ wt of fresh alum. All other chemicals used were laboratory grade.

EXPERIMENTAL PROCEDURE

Preparation of Metakaolin from raw Kankara kaolin clay

The raw clay was crushed using a mortar and pestle. The resultant product was then beneficiated by soaking in water and intermitent vigorious stirring for 3 days, after each day the spent water was replaced while sand particles were removed and discarded. The significance of removal of spent water is to faciliate the removal of soluble impurties. The kaolin suspension was then centrifuged and dried overnight at 120°C to remove free water [11]. The dried lump was crushed and screened with 315 microns sieve. The sieved clay powder was then weighed into crucibles and calcined in a muffle furnace at a temperature of 750°C for 2 hrs [2].

Dealumination of metakaolin using sulphuric acid

The dealumination of metakaolin ($Al_2Si_2O_7$) was performed by reacting 50 grammes of metakaolin with 168.03cm^3 of sulphuric acid of 96wt% (H_2SO_4) to give a 60 wt% acid solution [12]. A simplified chemical reaction for dealumination process is presented as Equation 29:

$$Al_2Si_2O_{7(s)} + 3H_2SO_{4(aq)} + 24H_2O \rightarrow Al_2(SO_4)_3.27H_2O_{(aq)} + 2SiO_2 \qquad (29)$$

Distilled water (184.27cm^3) was added to quench the reaction and to enhance the seperability of the alum ladden aliquot from the residual silica. The crystal yield obtained from 50ml of filtrate was observed to increase with decrease in temperature. This is in agreement with the established fact that the solubility of alum decreases at reduced temperatures [13,14]. The crystallization stage was achieved by cooling at -10^{o}C for 3 hours to initate the growth of alum crystals and resultant content is then filtered [2]. The hydrated alum crystals ($Al_2(SO_4)_3.27H_2O$) were gradually dried in an oven between 40^{o}C and 160^{o}C for 12 hrs. to enhance size reduction and seperation, after which the resultant sample is heated at 350^{o}C for 5 hours to remove the occluded acid and the chemically bonded water from the alum [9]. The dried alum was then ground and sieved with 315 microns [2]. Table 2 presents the compositional analysis for fresh alum and pretreated alums at 160^{o}C and 350^{o}C.

Calcination of the Pretreated Alum

40 grammes of ground alum in a crucible was calcined in a muffle furnace at 750^{o}C, 800^{o}C, 810^o C, 850^o C and 900^{o}C and for holding time intervals of 20,60, 120,150 and 180 minutes respectively. The residues were weighed and also subjected to X-ray flurorescence analysis after cooling to room temperature in a desiccator. A simplified decomposition reaction for aluminum sulphate is as shown in Equation 30.

$$Al_2(SO_4)_{3\,(s)} \rightarrow Al_2O_{3\,(s)} + SO_{3\,(g)} \qquad (30)$$

KINETIC PARAMETER ESTIMATION USING COATS-REDFERN MODEL

Kinetic parameter estimation using thermogravimetric data

The weight losses obtained were converted to conversion at different temperatures and time interval as shown in Table 5. The calculated conversion and temperature values were inputted into the Coats-Redfern model. Plot of $In\left[\frac{1-(1-X)^{1-n}}{T^2(1-n)}\right]$ vs $^1/_T$ were made. Regressing the left side of the above equation using the least square criteria for different values of n, the slope is –E/R and the intercept is equal to $-In\,^{AR}/_{\beta E}$; from these various plots, activation energy, E and the pre-exponential term, A were evaluated [9].

Discriminatory test for X ray Fluorescence results

The samples were then characterize using a Energy Dispersive -Xray Fluorescence machine to obtain the elemental composition by monitoring the extent of conversion of sulphate decomposition.

$$-In\left[\frac{g(X)}{T^2}\right] = In\left[\frac{1-(1-X)^{1-n}}{T^2(1-n)}\right] = \mathrm{In}\frac{AR}{\beta E}\left(1-\frac{2RT}{E}\right) + {}^{E}/_{RT} \quad (26)$$

Coats-Redfern model was adopted to estimate the kinetic parameters such as activation energy, pre-exponential factor and the order of the reaction were obtained by plotting a graph [9]

$$-In\left[\frac{g(X)}{T^2}\right] or\ In\left[\frac{1-(1-X)^{1-n}}{T^2(1-n)}\right]\ vs\ ^1/_T \qquad (31)$$

RESULTS AND DISCUSSION

The raw clay, beneficiated clay and metakaolin component analysis

From the results shown in Table 1, it was observed that the alumina content of the beneficiated clay increased significantly over the raw clay from 41.74 wt % to 43.01 wt. % while the silica content slightly decreased from 54.56 wt % to 53.95 wt %.

TABLE 1: CHEMICAL COMPOSITION OF RAW CLAY, BENEFICIATED CLAY AND METAKAOLIN

Component	Raw Clay %	Beneficiated clay %	Metakaolin %
Al_2O_3	41.74	43.01	44.87
SiO_2	54.56	53.95	52.41
CaO	0.44	0.34	0.32
Fe_2O_3	0.53	0.58	0.53
MgO	1.74	1.31	1.22
K_2O	0.71	0.56	0.47
Na_2O	0.04	0.05	0.04
TiO_2	0.10	0.07	0.07
Cr_2O_3	0.01	0.01	0.01
Mn_2O_3	0.02	0.02	0.01
NiO	0.01	0.03	0.02
CuO	0.08	0.06	0.03
ZnO	0.00	0.01	0.00

This could be attributed to the loss of organic material and free silicia respectively during the process of beneficiation. The color of the calcined kaolin changed from white to brick red indicating the presence of Fe^{3+} [15].

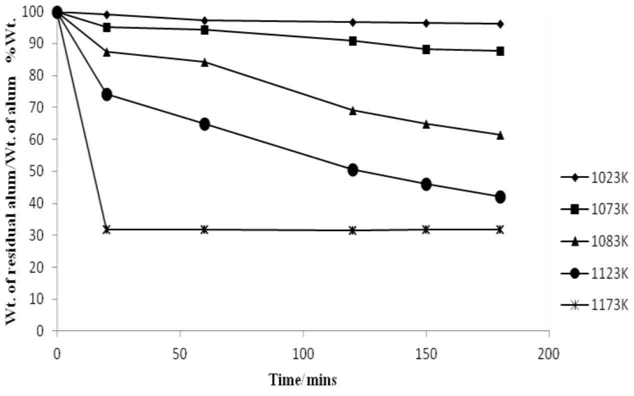

Fig.1: Residual weight analysis of calcined alum as a function of time

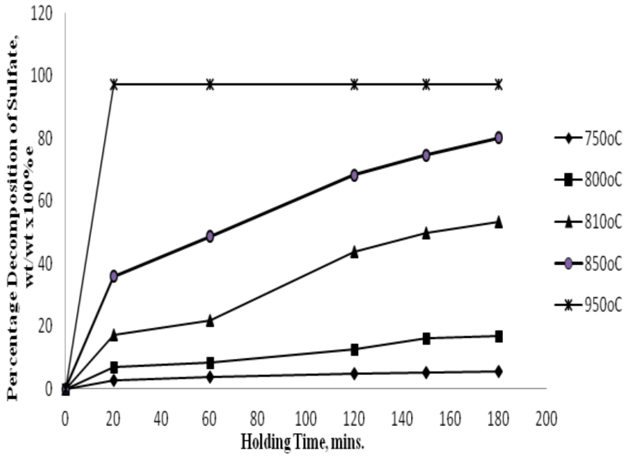

Figure 2: The Decomposition of Sulfate Component of the Alum as a Function of Temperature and Time

Effect of drying on alum

Drying at 160°C evidently was able to drive off the adsorbed free water on the alum and possibly part of the occluded water, while heating to 350°C was believed to be potent enough not only to eliminate the remaining occluded water but also the occluded excess acid as well. Table 2 showed these effects resulting in increase in concentration of alumina in the two heating steps; while SO_2 increased slightly in the first step, evidence of loss of free water and dropped partially in the second step, indicating loss due to occluded acid evacuation.

TABLE 2: ELEMENTAL COMPOSITION OF FRESH ALUM, THERMAL PRETREATED ALUMS AT 160°C AND 350°C

Components	Alum		
	Fresh Alum	*Dried at 160°C*	*Dried at 350°C*
Al_2O_3	8.41	8.7	16.02
SO_3	60.4	61.4	60.81
CaO	0.46	0.38	0.2
Fe_2O_3	0.18	0.24	0.14
MgO	0.17	0.02	0.31
K_2O	-	0.15	0.01
Na_2O	0.03	0.09	0.11
TiO_2	0.08	-	0.06
NiO	-	-	0.01

This observation is consistent with Moselhy et al. (1994) [9] differential thermal analysis (DTA) on a hydrated aluminium sulfate. The pretreated alum at 160°C comprised of about 8.41 wt/wt % of alumina which agrees with Alan et al, (2000) [16] that liquid alum contains about 8 wt/wt%.

Calcination of the partially dried alum (at 350°C)

The residual weight of the alum samples (in percentage of the initial quantity) obtained after calcination at different temperatures and time intervals are shown in Figure 1. Figure 2 shows the percentage of sulphate decomposed at various temperatures from thermogravimetric analysis. From Figures 1 and 2, it could be observed that the minimum residual weight of alum samples stood at 12.67g, while the maximum sulfate decomposition stood at 97.37%. The two figures clearly illustrated that as the temperature increased from 750 – 900°C, the sensitivity of the decomposition reaction increased, this is evident by steeper initial rates which flattens out as the reaction progressed from 20 mins. to 180 mins.

KINETIC PARAMETER ESTIMATION USING COATS-REDFERN MODEL

Kinetic parameter estimation from thermogravimetric data

The TGA data obtained from the decomposition of the pretreated alum were used to generate values to plot -*In* g(X) against 1/T, by varying the order n, between 0 and 2. Figure 3 is representative of such Coats-Redfern plots for estimating the kinetic and thermodynamic parameters.

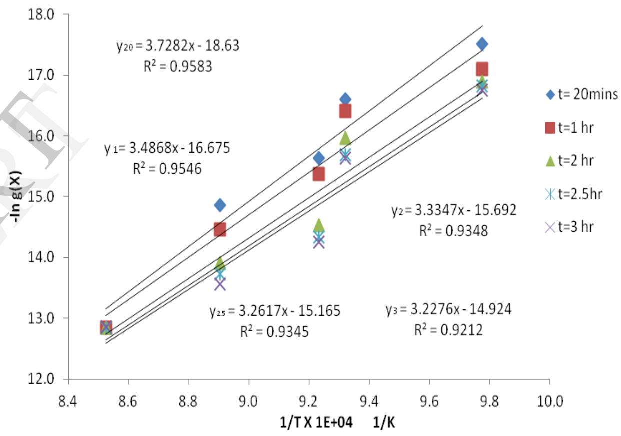

Fig. 3:Coats-Redfern plot for TGA at n=1.0

The summary of the regression analysis and the obtained kinetic parameters are shown in Table 3, indicating that reaction order of 1.3 for TGA gave the best average regression value of 0.9446 as compared with other orders within the range of 0 to 2 tested. The estimated average activation energy and pre-exponential factor corresponding to the reaction order 1.3 were 321.03 kJ/mol K and 2.57E+14 min^{-1} respectively.

TABLE 3: AVERAGE VALUES COMPARISION OF REGRESSION ANALYSIS AS OBTAINED FROM COATS-REDFERN METHOD OF ESTIMATING KINETIC PARAMETERS FROM TGA DATA

Order n	Equation y	**Kinetic parameters**		
		Regression value R^2	*Activation energy kJ/molK*	*Pre-exponential factor / mins*
0.0	y = 2.386x – 6.241	0.884	198.33	1.20E+08
0.5	y = 2.811x – 10.412	0.9178	233.69	8.28E+09
0.67	y = 2.992x – 12.168	0.9274	248.77	5.00E+10
1.0	y = 3.408x – 16.163	0.9407	283.13	3.01E+12
1.2	y = 3.702x – 18.983	0.9442	307.81	5.41E+13
1.3	y = 3.861x – 20.504	0.9446	321.03	2.57E+14
1.4	y = 3.863x – 22.097	0.94416	334.90	1.31E+15
1.5	y= 4.202x-23.7587	0.9272	349.37	7.18E+15
1.6	y= 4.383x-24.321	0.9409	364.43	4.2E+16
1.7	y=4.5709x-27.274	0.9384	380.03	2.61E+17
1.8	y=4.765x-29.118	0.9353	396.13	1.71E+18
1.9	y= 4.964x-31.02	0.9317	412.71	1.19E+19
2.0	y= 5.169x-32.97	0.9278	429.71	8.68E+19

Effect of reaction time on thermodynamic parameters' values

Table 4 revealed that as decomposition reaction progresses as a function of time while the order of the reaction was held constant at n= 1.3, the thermodynamic parameters: activation energy and pre-exponential factor experiences decrease in their values. This may be attributed to decrease in the barrier to heat and mass transfer due to increase in voidage in the sample matrix as the reaction progresses. The higher activation energy at the early stage of calcinations could also be attributed to the energy required for hydroxylation process coupled with sulfate decomposition, while at later times, sulfate decomposition being the sole reaction, which requires lesser energy for its transformation.

TABLE 4: TYPICAL VARIATION OF THE THERMODYNAMIC PARAMETERS ESTIMATED WITH REACTION HOLDING TIME FROM TGA DATA AT CONSTANT REACTION ORDER OF 1.3

Time/ mins	Equation y	Regression value R^2	Activation energy kJ/molK	Pre-exponential factor / mins
20	y = 4.0113x – 21.313	0.9410	333.50	5.79E+14
60	y = 3.7744x – 19.406	0.9432	313.80	8.09E+13
120	y = 3.6326x – 18.535	0.9461	302.01	3.26E+13
150	y = 3.5632x – 18.047	0.9513	296.24	1.96E+13
180	y = 3.5296x – 17.817	0.9415	293.45	1.54E+13

Kinetic parameter estimation from X-ray Fluorescence data

Figure 4 is a representative of the Coats-Redfern plots for estimating kinetic parameters for reaction orders of 0, 0.5, 1.0, 1.3 and 1.5 respectively from XRF conversion data on sulfate decomposition.

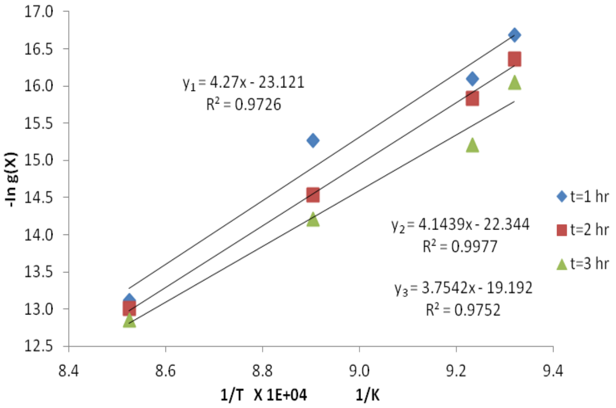

Fig. 4: Coats-Redfern plot for XRF at n=1.0

The summary of the regression analysis and the obtained reaction parameters are shown in Table 5, where order of 1.0 for XRF gave the best average regression value of 0.9818.

TABLE 5: AVERAGE VALUES COMPARISION OF REGRESSION ANALYSIS AS OBTAINED FROM COATS-REDFERN METHOD OF ESTIMATING KINETIC PARAMETERS FROM XRF DATA

Order N		**Kinetic parameters**		
	Equation y	*Regression value R^2*	*Activation energy kJ/molK*	*Pre-exponential factor / mins*
0.0	y = 2.431x – 6.400	0.8619	202.14	1.38E+08
0.5	y = 3.246x – 13.468	0.9698	269.85	2.48E+11
0.67	y = 3.494x – 15.744	0.9758	290.50	2.61E+12
1.0	y = 4.056x – 20.834	0.9818	337.22	5.27E+14
1.3	y = 4.509x – 25.266	0.9238	374.86	5.47E+16
1.4	y = 4.739x – 27.322	0.9244	394.01	4.79E+17
1.5	y = 5.114x – 30.281	0.9780	425.19	1.08E+19
1.6	y= 5.229x- 31.680	0.9241	434.70	4.78E+19
1.7	y=5.487x-33.976	0.9235	456.17	5.41E+20
1.8	y=5.753x-36.342	0.9225	478.34	6.59E+21
1.9	y=6.028x-38.776	0.9213	501.16	8.64E+22
2.0	y=6.592x-43.492	0.9731	548.04	1.28E+25

The estimated activation energy and pre-exponential factor for the best average regression analysis of order 1.0 were 337.22 kJ/mol K and 5.27E+14 min-1 respectively. Table 6 clearly shows that as the calcinations progressed, the activation energy and pre-exponential factor decreased as the reaction order was held at n=1. This reduction in the activation energy and frequency factor could be attributed to decrease in the diffusion barrier to heat and mass transfer resulting from increase in voidage as the reaction progresses.

TABLE 6: TYPICAL KINETIC PARAMETERS VARIATION WITH REACTION TIME FROM XRF DATA

Time / mins	*Equation y*	**Kinetic parameters**		
		Regression value R^2	Activation energy *kJ/molK*	*Pre-exponential factor / mins*
60	y = 4.270x – 16.42	0.9726	355.01	3.76E+15
120	y = 4.144x – 22.344	0.9977	344.52	1.68E+15
180	y = 3.754x – 19.192	0.9752	312.12	6.50E+13

From Table 7, the kinetic and thermodynamic parameters obtained from XRF data were slightly higher than those from TGA data. This can be attributed to the fact that X ray fluorescence analysis monitors the sulfate decomposition process only, while that of TGA is more or less average of several reactions including the effect of other metallic sulfates acting as impurities (Table 2) present in the prepared alum which could decrease the overall observed activation energy. It worth mentioning that the kinetic parameters obtained from the XRF data were in good agreement with that of Moselhy *et al.* from derivatograph data using the standard equipment, dynamic thermogravimetric method for data generation (n=1, E = 348 $kJmol^{-1}$ and A = 1.3E+16 s^{-1})

Validation of Coats-Redfern model

To validate the Coats-Redfern model, the assumption of the term $\left(1-\frac{2RT}{E}\right) \approx 1$. It was observed that after substituting typical activation energy , gas constant R, and temperature T. The fraction $2RT/E \leq 0.05$, was slightly insignificant resulting in a value of the term in the bracket approximately equal to 1. Thus validating the assumption.

III. CONCLUSION

From this study, it can be concluded that reaction orders of 1.0 and 1.3 were most acceptable for XRF data and TGA data respectively; having activation energy and pre-exponential factor of 337.22 kJ/molK (5.27E+14 min^{-1}) and 321.03 kJ/molK (2.57E+14 min^{-1}) respectively. The large activation energy indicates that the reaction is temperature sensitive. It was observed that as the calcination progressed while the reaction order was held constant there was a reduction in the activation energy and pre-exponential factor for both TGA and XRF results. This can be attributed to decrease in the diffusion barrier to heat and mass transfer most likely due to increase invoidage as the reaction progresses. Based on the assumption considered for Coats-Redfern model, the model was found to fit the rate data obtained satisfactorily.

REFERENCES

[1] Raw Materials Research and Development Council (2000), Raw Materials and Consumer industries in Nigeria, www.rmrdc.org.

[2] Abdul, B. Aderemi B.O. and Ahmed T.O. (2009): Production of alumina from Kankara kaolinite clay for electrical insulation applications. Int. J. Sci. & Techn. Research 6(1&2) pp107-114

Edomwonyi-Otu, L.C; Aderemi, B.O. and Ahmed A.S. (2010): Beneficiation of Kankara kaolin for alum production. Nig. J. of Eng. 16(2) 27-35

[3] Edomwonyi-Otu, L.C; Bawa, S.G. and Aderemi, B.O. (2010): Effect of Beneficiation of kaolin raw material on alumina yield and quality. Nig. J. of Eng. 16(2) 36-43

[4] Edomwonyi-Otu L.; Aderemi B.O and Ofoku, A.G. (2010): Studying the effect of calcination temperature and dealumination time on alum yield from Kankara kaolin. Afri. J. Nat. Sci. 13 pp 69 – 74

[5] Edomwonyi-Otu L.C.; Aderemi B.O.; Simo A. and Maaza M. (2012): Alum production from Nigerian kaolinite deposits. Int. J. Eng Res. in Africa 7 pp 13 – 19 Switzerland.

[6] Edomwonyi-Otu- L.C., Aderemi B.O., Ahmed A.S., Coville N.J. and Maaza M. (2013): Application of alum from Kankara kaolinite in catalysis: A preliminary report. Ceramic Transactions 240 pp 167 – 174

[7] Edomwonyi-Otu- L.C., Aderemi B.O., Ahmed A.S., Coville N.J. and Maaza M. Influence of thermal treatment on Kankara kaolinite Opticon1826 15(5) 1-5 (2013)

[8] Moselhy H.J.; Madarasz, G; Pokol, S; Pungor, E.(1994). Aluminum Sulphate hydrates: Kinetics of the Thermal Decomposition of Aluminum Sulphate using different calculation methods' Journal of Thermal Analysis 41:1,25.

[9] Coats, A. W., Redfern, J. P. (1964): Kinetic parameters from Thermogravimetric data. Nature Vol. 201. pp. 68–69.

[10] Aderemi, B.O, Oloro, E.F, Joseph, D, Oludipe, J. (2001) Kinetics of the Dealumination of Kankara Kaolin Clay, NJE vol.9 No1, pp 40-44.

[11] Aderemi, B.O. and Oludipe, J.O. (2000). Dealumination of Kankara Kaolin Clay–Development of Governing Rate Equation. Nig. J. of Eng. 8(2) 22-30

[12] MacZura G, Goodboy, K.P.; Koenig, J.J. (1978) Aluminium Sulfate and Alums in Kirk-Othmer (Ed), Encyclopedia of Chemical Technology, Wiley Interscience New York, Vol 2, pp 245-250.

[13] Perry R. H., Green, D. W. (1997) Perry's Chemical Engineering Handbook. McGraw-Hill Book Co. Pp 28 -36, 28-43.

[14] Vogel A, I. (1999) Quantitative Inorganic Chemical Analysis. 4th edition pp.354.

[15] Alan C., Ratnayaka D., Malcolm J. B., (2000), Water supply-Technology & Engineering pp. 676.